Available at: http://www.ictp.it/~pub_off IC/2006/024

United Nations Educational Scientific and Cultural Organization
and
International Atomic Energy Agency

THE ABDUS SALAM INTERNATIONAL CENTRE FOR THEORETICAL PHYSICS

MECHANISM OF PHOTONIC BAND GAP, OPTICAL PROPERTIES, TUNING AND APPLICATIONS

Akhilesh Tiwari
Department of Physics and Electronics, D. A-V. College, 119/91, Darshanpurwa, Kanpur-208012, India

and

Manoj Johri[1]
Department of Physics and Electronics, D. A-V. College, 119/91, Darshanpurwa, Kanpur-208012, India
and
The Abdus Salam International Centre for Theoretical Physics, Trieste, Italy.

Abstract

Mechanism of occurrence of Photonic Band Gap (PBG) is presented for 3-D structure using close packed face centered cubic lattice. Concepts and our work, specifically optical properties of 3-D photonic crystal, relative width, filling fraction, effective refractive index, alternative mechanism of photonic band gap scattering strength and dielectric contrast, effect of fluctuations and minimum refractive index contrast, are reported. The temperature tuning and anisotropy of nematic and ferroelectric liquid crystal infiltrated opal for different phase transitions are given. Effective dielectric constant with filling fraction using Maxwell Garnet theory (MG), multiple modified Maxwell Garnet (MMMG) and Effective Medium theory (EM) and results are compared with experiment to understand the occurrence of PBG. Our calculations of Lamb shifts including fluctuations are given and compared with those of literature values. We have also done band structure calculations including anisotropy and compared isotropic characteristic of liquid crystal. A possibility of lowest refractive index contrast useful for the fabrication of PBG is given. Our calculations for relative width as a function of refractive index contrast are reported and comparisons with existing theoretical and experimental optimal values are briefed. Applications of photonic crystals are summarized. The investigations conducted on PBG materials and reported here may pave the way for understanding the challenges in the field of PBG.

MIRAMARE – TRIESTE

May 2006

[1] Junior Associate of ICTP.

Introduction

The condensed matter physics of the 20th century has given two important technological breakthroughs; firstly the Electronic Localization[1], which led to the semiconductor revolution in electronic industry and secondly the invention of Laser. However, with the use of the laser everything became possible except the search of any real material that could micro-manipulate the flow of light in the same way as the semiconductor does to electrons. The discovery of photonic band gap material is one of the frontiers in science and technology, so that all functions are possible by photons as are performed by electrons. The analogy of forbidden gap in semiconductor of electrons with the photonic band gap in semiconductor of light is another example in the direction of interpreting these gaps. Purcell[2] discovered that with the presence of a mirror one could alter radiation properties of an electromagnetic dipole. The principle of complete inhibition of spontaneous emission from an atom or molecule resulted from the ideas of Purcell[2] which are the direct corollary of the work of Anderson strong localization[1]. John worked on the caging of light[3] and gave fundamental optical principle namely localization of photons[4]. Yablonovitch[5] was engaged in work on reducing the losses due to spontaneous emission in lasers. He postulated another fundamental optical principle of Inhibition of Spontaneous Emission. Both these researchers[4,5] agreed simultaneously to propose photonic band gap for flow of photons similar to forbidden band gap in semiconductor for electron flow. The theoretical proposition[4] of minimum density of states giving a pseudophotonic band gap including the effect of disorders (fluctuations) was experimentally verified by Yablonovitch and Gmitter[6]. The researchers[6] did not show the degeneracy at the W-point of the Brillouin Zone (BZ) considering close packed face centered cubic (fcc) lattice and he erroneously reported complete photonic band gap. Ho et al[7] resolved the problem of degeneracy at W-point of the BZ by considering the diamond lattice and proposed a complete photonic band gap (CPBG) and it was experimentally verified by Yablonovitch et al[8]. In an analogy with the semiconductors one can use doping process in these structures by locally adding or removing materials i.e. by creating a defect[9]. It is possible to demonstrate the localized states in the CPBG. The type of dopents is also important, the addition of material leads to a donor type defect and it is near the conduction band (CB) edge of the crystal structure, while removal of material corresponds to an acceptor type defect and it is near the valence band (VB). Such structures are called as semiconductor of light (or photonic crystal or electromagnetic crystal or photonic band gap material). John

and Wang[10,11] used quantum electrodynamics and collective phenomenon in a photonic band gap separating VB and CB by atomic impurity band as a result of photon atom bound state.

There have been many structures for one dimension (1-D), two dimensions (2-D) and three dimensions (3-D) photonic band gap materials as given[12] in Figure 1. For one dimension case we have two types of behaviour (i) wavelength in the band gap and (ii) wavelength not in the band gap. In the former case a wave incident on a band gap material (Figure 1a) partially reflects off each layer of the structure (Figure 1b). The reflected waves are in phase and reinforce one another. They combine with the incident wave to produce a standing wave (Figure 1c) that does not travel through the material. For wavelength not in band gap, at a wavelength outside the band gap (Figure 1d), the reflected waves are out of phase and cancel out one another (Figure 1e). The light propagates through the material only slightly attenuated (Figure 1f). For a two dimensional band gaps each unit cell of the structure (Figure 2a) produces reflected waves and refracted waves that must combine to cancel out the incoming wave (Figure 2b) no matter what direction it is travelling (Figure 2c). The waves are not shown in these figures. For three-dimensional geometry the band gap material works like two-dimensional cases. Diamond's tetrahedral configuration (Figure 3a) is the most effective geometry for making three dimensional band gap materials. This geometry occurs in a disguised form in 'Yablonovite'. The track of logs (Figure 3b) and this design (Figure 3c) shows silicon dioxide channels (light shade) in silicon (dark shade). The scattered structure (Figure 3d) is a rare example that has different underlying symmetry but it has only a small band gap. Johri and his coworkers[13-18] have studied 3-D photonic crystal structures and various research groups have proposed 3-D photonic crystal; some of important ones are given for ready reference in Figure 4. The theoretical methods are basically categorized as plane wave expansion method (PWE), transfer matrix method (TMM) and finite difference time domain technique (FDTD) while experimental methods include etching technique, layer by layer fabrication, woodpile structure and colloids etc.

We report our results for relative width, filling fraction and effective refractive index. Alternative mechanism of photonic band gap using scattering strength dielectric contrast, and the effect of fluctuations, minimum refractive index contrast are considered. The tuning of photonic band gaps for liquid crystal infiltrated synthetic opal is given. A calculation of variation of effective dielectric constant using different theoretical models as a function of filling fraction is given and a comparison is made with existing experimental data. We have

also calculated relative width as a function of refractive index and optimal values are reported in comparison to existing theoretical and experimental data. Theoretical formulation for Lamb Shift is given considering fluctuations and anisotropic model. Band structure calculations and effect of anisotropy for tuning of PBG are also given. The impact of photonic crystals and applications is summarized.

Optical Properties of Photonic Band Gap Material

Relative Width

The key properties are refractive index contrast, relative width, filling fraction and tuning of the photonic band gap using mechanical, magnetic, temperature variational and potential anisotropy variation methods. Minimum density of states, refractive index difference minimum and scattering strength have been cited for the mechanism of occurrence of photonic band gap. We consider relative width variation with refractive index for the sake of comparison in Figure (3). The method of John[4] has been used to derive an expression for relative width and the final expression obtained is

$$\Delta\omega/\omega_0 = 2[\{\sqrt{(3n_a^2+2n_b^2)} - \sqrt{(2n_a^2+3n_b^2)}\} / \{\sqrt{(3n_a^2+2n_b^2)} + \sqrt{(2n_a^2+3n_b^2)}\}] \quad (1)$$

Filling Fraction

The isotropic model[4] gives following expression for filling fraction

$$f_{opt} = 1/2n. \quad (2)$$

For n=3.5 one gets $f_{opt} \approx 0.14$. The volume-filling fraction is usually defined as the ratio of volume of sphere to the volume of cell, i.e.,

$$f = 4\pi/3(R_s/l^3), \quad (3)$$

where R_s is the radius of sphere and l is the unit cube length. The value f=0.74 corresponds to close packing of spheres beyond which overlapping occurs. The optimum value of filling fraction given in eq. (2) could be written for dielectric sphere in spherical air atoms i.e. with dielectric constant ε_a and ε_b respectively

$$f_{opt} = n_b/(n_a+n_b) \quad (4)$$

Effective Refractive Index

The calculation of n_{eff} is of paramount importance in band structure calculations because it is related to the slope of the lowest two bands and to the accuracy of the first gap. The effective refractive index can be measured by measuring effective dielectric constant of a capacitor made of two large parallel plates sandwiching the heterogeneous medium, i.e.,

$$n_{eff} = \sqrt{\varepsilon_{eff}} = [\lim_{A,d\to\infty} \frac{d}{A} C(A,d)]^{1/2}, \quad (5)$$

Using $k^2 = (5/12)\, G^2$ for W-point of the BZ and John[4] model we have obtained following expression of effective refractive index

$$(n_{eff})_w = 2(5)^{-1/2} [(3n_a^2 + 2n_b^2)^{1/2} + (2n_a^2 + 3n_b^2)^{1/2}]. \quad (6)$$

The calculations of n_{eff} were done by several authors[19-20] using average value of the lowest four frequencies at the X-point of the BZ in the long wavelength approximation. Yablonovitch and Gmitter[6] modified refractive index with volume filling fraction by simple linear interpolation using eq. (2) and extrapolation was done up to f =1.0 for their expression of n_{eff} i.e.,

$$(n_{eff})_x = (2\,\pi/a\,\omega_x)c, \quad (7)$$

where c is the speed of light, ω_x is the centre frequency for X- point of the BZ and 'a' is the fcc unit cube length.

Zhang and Satpathy[21] used following relation for n_{eff} in the long wavelength limit

$$(n_{eff})_x = \lim_{k\to 0} \frac{c}{(d\omega_x/dk)}, \quad (8)$$

where k is the propagation vector and $(d\omega_x/dk)$ is the group velocity. Leung and Liu[19] have assumed the slope of the line of the dispersion curves originating from the point Γ of the BZ as $n_b/(n_{eff})_x$. For infiltration of one material into the other the effective refractive index can be approximately expressed as follows

$$(n_{eff})_{air} = [f^2 \times 1^2 + (1\text{-}f)\, n_b^2]^{1/2}, \quad (9)$$

$$(n_{eff})_{diel} = [f \times n_a^2 + (1\text{-}f)\, 1^2]^{1/2}, \quad (10)$$

where volume filling fraction is found by using eq. (3).

Alternative Scattering Strength Mechanism of the PBG, Effect of Fluctuations, Minimum Dielectric Contrast and Temperature Tuning of PBG

John[4] has given a dispersion relation in terms of the small deviation **q** of the wave vector **k** from the point $\mathbf{k_0}$ on the Bragg plane for which $k_0^2 = G^2/(1+\varepsilon_0/\varepsilon_1)$. There are three components of **q,** i.e., q_1, q_2 and q_3. The third component q_3 tangent to the Bragg plane does not enter in the dispersion relation

$$\omega^2/c^2 = E_c + A_1 q_1^2 + A_2 q_2^2, \tag{11}$$

where $E_c = 2k_0^2 / (\varepsilon_0 + \varepsilon_1)$. (12)

$$A_1 = (2/\varepsilon_1)\,[(\varepsilon_0^2 + \varepsilon_1^2)/ (\varepsilon_0^2 - \varepsilon_1^2)]. \tag{13}$$

$$A_2 = (2/\varepsilon_1)[3-\varepsilon_0/\varepsilon_1)/(\varepsilon_0/\varepsilon_1 + 1)]. \tag{14}$$

In eq. (8) we have separated the total dielectric constant $\varepsilon(\mathbf{x})$ into its average value ε_0 and spatially fluctuating part $\varepsilon_{fluct}(\mathbf{x})$. This fluctuating component plays a role analogous to the random potential and it scatters the electromagnetic waves. It is scattering component. The condition $\varepsilon_0 + \varepsilon_{fluct}(\mathbf{x})>0$ everywhere translates into the requirement that the energy eigen value be always greater than the effective potential $|(\omega^2/c^2)\ \varepsilon_{fluct}(\mathbf{x})|$. The terms ε_0 and $\varepsilon_{fluct}(\mathbf{x})$ have been defined elsewhere[4]. The ε_0 corresponds to non- scattering component. The scattering strength is defined as the ratio of scattering component to the non-scattering component in crude sense. The scattering strength is a measure of deviation from the free photon condition. To derive scattering strength we write, from John[4] theory

$$-\nabla^2\mathbf{E} + \nabla(\nabla.\mathbf{E}) - (\omega^2/c^2)\ \varepsilon(\mathbf{x})\ \mathbf{E} = 0, \tag{15}$$

where $\varepsilon(\mathbf{x}) = \varepsilon_0 + \varepsilon_{fluct}(\mathbf{x}) = \varepsilon_0 + \{\varepsilon_1(\mathbf{x}) + V(\mathbf{x})\}$. (16)

Scattering strength is

$$\varepsilon_r(\mathbf{x}) = \varepsilon_{fluct}(\mathbf{x})/ \varepsilon_0, \tag{17}$$

which may be written as,

$$\varepsilon_r(\mathbf{x}) = (\varepsilon_1(\mathbf{x}) + V(\mathbf{x}))/ \varepsilon_0, \tag{18}$$

Under special circumstances we define scattering strength as,

$$\varepsilon_r \approx \varepsilon_1/\varepsilon_0 = (\varepsilon_a - \varepsilon_b)/(\varepsilon_a + \varepsilon_b), \tag{19}$$

But this equation is true only for $\varepsilon_1/\varepsilon_0 > 1/3$ under the John's idea[4] for $\varepsilon_1/\varepsilon_0=1/3$ we get $n_b/n_a=0.707$ but for value of $\varepsilon_r=1$, eq. (19) is not applicable and we get $\varepsilon_b=0$ as such. However, we assume geometrical mean (GM) of ε_a and ε_b because for large values of dielectric contrast only GM is appropriate rather than arithmetical average. We can get

optimum value of ε_r from the following equation by replacing $(\varepsilon_a+\varepsilon_b)/2$ by $\varepsilon_0=(\varepsilon_a\varepsilon_b)^{1/2}$ for non linear characteristics. Therefore eq. (19) is reduced to

$$(\varepsilon_r)_{opt} = (\varepsilon_a - \varepsilon_b)/2\sqrt{\varepsilon_a\varepsilon_b}\,. \tag{20}$$

To modify the decomposition[4] of $\varepsilon(\mathbf{x})$ we replace ε_0 by effective spatial average$<\varepsilon>$, i.e.,

$$\varepsilon(\mathbf{x}) = <\varepsilon> + \varepsilon_{fluct}(\mathbf{x}),$$

$$= \text{Non-scattering component} + \text{Scattering component} \tag{21}$$

The scattering strength $\varepsilon_r(\mathbf{x})$ is the ratio of scattering to non-scattering component i.e.,

$$\varepsilon_r(\mathbf{x}) = \varepsilon_{fluct}(\mathbf{x})/<\varepsilon>, \tag{22}$$

The spatial average $<\varepsilon>$ in eq. (22) may be defined as follows

$$<\varepsilon> = \frac{\int_{ws}\varepsilon(\mathbf{x})\,d\mathbf{x}}{V_{cell}}\,, \tag{23}$$

where 'ws' stands for Wigner Sietz cell and V_{cell} is the volume of the primitive cell of the lattice, where $<\varepsilon>$ is space average part responsible for no scattering or forward scattering while $\varepsilon_{fluct}(\mathbf{x})$ gives off-axis scattering (or scattering). $\varepsilon_{fluct}(\mathbf{x})$ is solely responsible for the deviation from the free photon problem. From eq. (21) and (22) we get the scattering strength as $\varepsilon_r(\mathbf{x}) = (\varepsilon(\mathbf{x})/<\varepsilon>) - 1,$ (24)

For a periodic array of dielectric spheres, each of radius R_s and dielectric constant ε_a, embedded in a background (host) medium ε_b one can write to a first approximation

$$\varepsilon(\mathbf{x}) \approx <\varepsilon^2> = f\varepsilon_a^2 + (1-f)\varepsilon_b^2. \tag{25}$$

and also

$$<\varepsilon>^2 = c^2/<c>^2 = [f\varepsilon_a + (1-f)\varepsilon_b]^2, \tag{26}$$

where c is speed of light. We consider ε_r as the measure of deviation from the free photon problem and it can now be expressed as

$$\varepsilon_r = [(<\varepsilon^2>/<\varepsilon>^2) - 1]^{1/2}. \tag{27}$$

For spherical air atom (n_b = varied, n_a=1) we get ε_r as

$$\varepsilon_r = [\{f\times 1^4 + (1-f)\,n_b^4\}/\{f\times 1^2 + (1-f)\times n_b^2\}^2 - 1]^{1/2}. \tag{28}$$

While for dielectric sphere (n_b=1, n_a = varied) the expression for ε_r is

$$\varepsilon_r = [\{f\times n_a^4 + (1-f)\times 1^4\}/\{f\times n_a^2 + (1-f)\times 1^2\}^2 - 1]^{1/2}. \tag{29}$$

For ε_r=1 we get a new expression for dielectric contrast

$$\varepsilon_a/\varepsilon_b = [\{(1-f)/(1-2f)\}\{2 \mp 1/\sqrt{(f(1-f))}\}], \tag{30}$$

where f is computed by the ratio of the volume of a component to the total volume of the composite system. A plot of $\varepsilon_a/\varepsilon_b$ versus f is given in Figure 5.

We propose an alternative mechanism in this work to assure a photonic band gap arising as a result of overlapping of gaps in addition to existing one of density of state minimum. The proposed criterion chosen is threshold value of effective refractive index to optimize scattering strength. The effective refractive index is defined by $<\varepsilon>$ may be minimized by putting in eq. (26) the following condition

$$f\varepsilon_a = (1-f)\,\varepsilon_b, \tag{31}$$

i.e., the filling fraction for optimum value for ε_r and minimum value of effective refractive index $(n_{eff})_{min}$ is given below

$$f_{opt} = \varepsilon_b / (\varepsilon_a + \varepsilon_b) \qquad \text{and} \quad (1- f_{opt}) = \varepsilon_a/(\varepsilon_a+\varepsilon_b), \tag{32}$$

This value of f_{opt} also provides optimum value of ε_{ropt} when eq. (20) obtained in this work is used. The physical basis for eq. (31) is that the filling fraction must be a factor which when multiplied by the sum of the dielectric constant of the dielectric sphere and the back ground amounts to the dielectric constant of the background or $2f\sqrt{(\varepsilon_a\varepsilon_b)}= \varepsilon_b$, i.e., $f=(1/2)\sqrt{(\varepsilon_b /\varepsilon_a)}$ or dielectric contrast is equal to $4f^2$. The optimum value of filling fraction in eq. (2) can be obtained by our present approach i.e. $2fn_an_b =n_b$ for $n_a=n$.

The density of state minimum gives a pseudogap. The minimum refractive index difference may also assure the occurrence of the photonic band gap combined with density of states minimum as it leads to overlapping of gaps for different (BZ). We intend to reanalyze the situation for the occurrence of the photonic band gap taking into consideration effective dielectric constant for long wavelength limit, mechanism of minimum dielectric constant difference, optimum scattering strength and overlapping of gaps for different points of BZ. The expressions of relative width have been derived and the effective dielectric constant for heterogeneous medium has been experimentally observed by sandwitching the medium.

Using eq. (19) and (20) the relative width at W-point of the BZ is

$$\Delta\omega/\omega_w= 2[\{(5-\varepsilon_{ropt})^{-1/2} - (5 + \varepsilon_{ropt})^{-1/2}\}/\{(5-\varepsilon_{ropt})^{-1/2} + (5 + \varepsilon_{ropt})^{-1/2}\}] \tag{33}$$

where ratio of propagation vector (**k**) and reciprocal vector (**G**) is $(5/12)^{1/2}$. The value of relative width for $\varepsilon_{ropt}=1$ is 20.2%. The overlapping of gaps is also crucial to assure existence of the PBG. Let us consider X- and L- point of the BZ which differ in frequency such that $\nu_x/\nu_L = (2/\sqrt{3})$ giving a gap $(\nu_x-\nu_L)$ which could be normalized to one of these frequencies therefore $\Delta\nu/\nu_x$ where $\Delta\nu=(\nu_x -\nu_L)$. For overlapping of gaps we get $(\Delta\omega/\omega_w)$ equal to $\Delta\omega/\omega_x$, i.e.,

$$(1-\sqrt{3}/2)=2[\{(5\varepsilon_0-\varepsilon_1)^{-1/2}-(5\varepsilon_0+\varepsilon_1)^{-1/2}\}/\{(5\varepsilon_0-\varepsilon_1)^{-1/2} + (5\varepsilon_0+ \varepsilon_1)^{-1/2}\}] \tag{34}$$

which gives $\varepsilon_1/\varepsilon_0 \approx 0.335$ and it is just more than 1/3 as assumed by John[4] for the occurrence of this pseudo PBG. The present work provides useful ideas about variation of effective dielectric constant as a function of filling fraction. The occurrence of the PBG could be assured by the mechanisms of minimum density of states, optimum scattering strength refractive index difference minimum and the overlapping of gaps for different points of the BZ.

Temperature Tuning

We have done calculations for relative width of nematic liquid crystal ZLI-1132 and smectic ferroelectric liquid crystal (R)-4′-(1-methoxycarbonyl-ethoxy)-phenyl-4-[4-(n-octyloxy)phenyl]benzoate (1MC1EPOPB) synthetic opal (SiO_2) infiltrated with liquid crystal as a function of temperature for the occurrence of pseudogap are reported for the W-point in the Brillouin zone. A new expression for relative width as function of refractive index for synthetic opal infiltrated with liquid crystal is proposed. The elative width ($\Delta\omega/\omega_c$) of the stop band is

$$\frac{\Delta\omega}{\omega_c} = \frac{2[(3n_a^2 + 2n_b^2)^{1/2} - (2n_a^2 + 3n_b^2)^{1/2}]}{[(2n_a^2 + 3n_b^2)^{1/2} + (3n_a^2 + 2n_b^2)^{1/2}]}, \quad (35)$$

Calculation of Effective Dielectric Constant Using Different Models

Lorentz-Lorentz[22], Brugmann's approach[23], Korringa, Kohn and Rostoker (KKR) band structure procedure[24], Busch and Soukoulis[25] effective medium theory have discussed the effective dielectric constant. We use Maxwell Garnet (MG)[26], Multiple Modified Maxwell Garnet (MMMG)[27]. The expressions used are

$$<\varepsilon>_{MG} = \varepsilon_b [2\varepsilon_b + \varepsilon_a + 2f\,|\,\varepsilon_a-\varepsilon_b\,|\,/\,[2\varepsilon_b + \varepsilon_a\, f\,|\,\varepsilon_a-\varepsilon_b\,|\,] \quad (36)$$

$$<\varepsilon>_{MMMG} = \varepsilon_b[\varepsilon_b + [P^E\,(1-f) + f\,]\,|\,(\varepsilon_a-\varepsilon_b)\,|\,]/[\varepsilon_b + P^E(1-f)\,|\,(\varepsilon_a-\varepsilon_b)\,|\,] \quad (37)$$

$$3(1-f)\,/\,2+\varepsilon_b/\,<\varepsilon>_{EM} + 3f\,/\,2+\varepsilon_a\,/\,<\varepsilon>_{EM} = 1 \quad (38)$$

where f is the volume filling fraction, ε_a is dielectric constant of dielectric material while ε_b is that for the surrounding medium. The composite material may be of two types i.e. dielectric sphere ($\varepsilon_a = \varepsilon,\ \varepsilon_b = 1$) and dielectric air atom ($\varepsilon_a = 1,\ \varepsilon_b = \varepsilon$). The P^E is the depolarizing factor, which has been taken $\approx 1/3$ in the present calculation. The present variation of effective

dielectric constant versus filling fraction is given in Figure 8 for dielectric sphere and for spherical air atom using different approaches.

Calculation of Relative Width versus Refractive Index and Optimal Values

Theoretical Formulation for Lamb Shift

Lamb and Rutherford[28] detected ordinary Lamb Shift of the $2s_{1/2}$ level using microwave technique. It has been shown[10,11,29] that near a band edge, the dressing of the photons with a finite effective mass becomes strong enough to split the atomic level by an observable amount. An expression was given[10,11,29] for anomalous Lamb shift for the case of hydrogen, which affects the odd parity $2p_{1/2}$ and not the even parity $2s_{1/2}$. They introduced a simple isotropic model Hamiltonian for electromagnetic waves in a three dimensional periodic dielectric medium and they found anomalous splitting of $2p_{1/2}$ level comparable to the ordinary Lamb Shift of $2s_{1/2}$ level.

The anisotropic model[4] used in the present calculation gives the following dispersion relation

$$E - E_1 \equiv \alpha \left| \mathbf{P}_{10} \right|^2 \frac{E \int d^3\mathbf{k}}{c^2 m^2} (1/\omega_k^2 \, (E/\hbar - \omega_k) \tag{39}$$

We define E as $(\omega_k/c)^2$, where c is speed of light and ω_k is angular frequency for propagation vector k. The value of ω_k becomes singular (ω_c) near conduction band edge i.e. $E_1 = (\omega_c/c)^2$ for $k = k_0$. The p_{10} is the known dominant dipole matrix element for ground state, α is the fine structure constant. When E_1 is close to a conduction edge frequency i.e. (ω_c/c) and $\left| P_{10} \right|^2 \neq 0$ the quantum electrodynamic interaction is so strong that atomic level $2p_{12}$ of hydrogen is splitted as a doublet. We consider that anisotropic dispersion relation as a function of fluctuations q_1, and q_2 as given in eq. (11).

From eqs.(11), (12), (13) and (14) the Lamb shift $z=(E-\hbar\tilde{\omega}_c)/\hbar\omega_c$ is obtained[29] by considering integration limits as q_1/G and q_2/G in eq.(39) i.e.

$$z \cong \alpha \left| P_{10} \right|^2 \frac{\pi[A_2/2]^{1/2} \left| G/\omega_c \right|^3}{m^2 c^2} g_1(z) \tag{40}$$

where: $g_1(z) \sim \pi[(c^2G^2/2\omega_c^2)^{-1} (A_1A_2)^{1/2} \ln \left| z \right|$ (41)

Using dielectric contrast $\varepsilon_0/\varepsilon_1$as a function of different refractive indices, we can get

$$z/\ln z = 3\pi\varepsilon_0(2\varepsilon_1)^{1/2}(1+\varepsilon_1/\varepsilon_0)[(1-\varepsilon_1^2/\varepsilon_0^2)/(1+\varepsilon_1^2/\varepsilon_0^2)]^{1/2} \times 10^{-8} \quad (42)$$

We also calculate z/lnz directly by considering definition of Lamb shift as $z = (E-E_c)/E_c$ with $E = \omega_k^2/c^2$ and $E_c = \omega_c^2/c^2$ then

$$z/\ln z = \{(E-E_c)/E_c\} \,/\, \ln\{(E-E_c)/E_c\} \quad (43)$$

The value of ω_k is computed using the dispersion relation for p-polarization in the Bragg plane such that the phase space for propagation near a conduction band edge is defined by the frequency (ω_c) satisfying the criteria for the occurrence of the photonic band gap as $(\varepsilon_1/\varepsilon_0) > 1/3$.

$$\omega_k/c = k\,(\varepsilon_0 \pm \varepsilon_1 \,\left|\, 1-G^2/2k^2 \right|)^{-1/2} \quad (44)$$

Consideration of eq. (44) with +ve and –ve sign as $(\omega_k/c)_I$ and $(\omega_k/c)_{II}$ respectively, we get

$$(\omega_k/c)_I = (2\varepsilon_1)^{1/2}\, G/(\varepsilon_0+\varepsilon_1) \quad (45)$$

$$(\omega_k/c)_{II} = (2\varepsilon_1)^{1/2}\, G/\,\{(\varepsilon_0+\varepsilon_1)(\,3\varepsilon_0-\varepsilon_1)\}^{1/2} \quad (46)$$

Calculation of Band Structure and Anisotropic Effect

We have also made an effort for the tuning of the photonic band gap other than the temperature variation mentioned here above, this have been done by changing the anisotropy in liquid crystal infiltrated in opal. We are reporting only the effect of two liquid crystals infiltrated in opal by considering the bulk dielectric constant obtained from parallel and perpendicular dielectric constants. Band structure of the opal[30] given in Figure 10(a) (n_{opal} =1.46) infiltrated with liquid crystal ($n_{LC} = (n^e_{LC} + 2n^0_{LC})/3$ = 1.584, n^e_{LC} =1.706, n^0_{LC} =1.522), when each director of the nematic axis turns at random, i.e. isotropic material and in Figure 10(b) when the director of the nematic axis turns perpendicular to (1, 1, 1) director of the light. We have done band structure calculation for the purpose to know the effects of increasing the number of plane waves and decreasing the error. The time required is the important parameter, which also required and enhanced the cost. The Figure 11 of band structure for silicium polymer calculated using 671 plane waves. The calculation indicates that for most accurate band structure calculation is yet to be done, other than the other workers have done, needing a computer, which may take insignificant time and it may be better than even the super computer which takes an hour. This may lead to an important

application for photonic crystal for principles leading to the prepositions of a quantum computer.

Applications of Photonic Crystal

The initial commercial and military applications are in the realm of handheld wireless communications and global- positioning system antennas using the high-impedance ground plane structure; The optical applications are of more long range, but we can expect an impact on white pigments that are ubiquitous in our surroundings; on optical signal processing; Light emitting diodes for both commercial and military use; Low threshold optical switches; Optical transistors for optical communication; High speed optical computers (or quantum computers); Ultra low noise coherent light sources; Fibre optic phone line; Optical bistability may provide a very low threshold high speed optical switch; Multipurpose photonic integrated circuit to work at μm and sub μm scale; Bandwidth of dielectric material of the order THz (Tera hertz); The same photonic crystal may be used for different frequency as Maxwell's equations have no fundamental length scale; The goal is to fabricate photonic crystal for telecommunication of 1.5 μm and lattice constant (≈ 0.5 μm); Working memory of quantum computer may be 10^6 Gbytes; Quantum computer may do calculations in feta seconds. One million calculations could be done in this time, before the quantum information falls. This cannot be done by sophisticated super computer. Materials for photonic crystals; Metals, Metalo-dielectric photonic crystal; Synthetic opals infiltrated with the unit materials Si, Ge, Gap, TiO_2, CdSe, GaAs, InP, InGaAsP, CdS, SiO_2+LC and Si+SiO_2 etc. Applications for Different Dimensional Photonic Crystal

Device	Description	Status
Ultra White Pigment	Incomplete 3-D band gap Material, usually patterned as opal structure	Demonstrated (Manufacturing methods under development)
Photonic Integrated Ckts	2-D thin films can be patterned like conventional integrated circuits to make channel filters, modulators, couplers and so on.	Under development
Nanoscopic Lasers	World tiniest optical Cavities and tiniest laser formed in a thin film 2-D band gap material.	Demonstrated (in the lab)
Radio-Frequency Antennas, Reflectors	Uses as inductors and capacitors in place of ordinary dielectric material	Demonstrated (But must compete with other Methods- Antennas & Magnetic Resonance Imaging)
Light Emitting Diodes	PBG structures can extract light very efficiently (better than 50%)	Demonstrated but must compete with other methods
Optical Fibers	2-D band gap materials Stretched along IIIrd Direction	Commercialized

In summary we can mention that the full practical impact of PBG is yet to be seen.

Results and Discussions

A brief review is given on the development of photonic crystal and its optical properties along with photonic band gap in different dimensions. The theoretical concepts filling fraction, effective refractive index and our calculations for relative width as a function of refractive index are given in Figure 5. Comparison with the results of Yablonovitch et al[8] and Ho et al[7] have been made. A good agreement between the experimental result[8] has been found with our calculated results at refractive index 3.6. The optical values of refractive index

contrast, volume-filling fraction, size of the gap in 3-D fcc dielectric structure by various researchers are given in the Table 1. We have also calculated the coefficients which occurred in fluctuating potential in eq. (11) and a plot is given as a function of refractive index as demonstrated in Figure 6. We derived a new relation for the dielectric contrast for eq.(30) and the variation of refractive index contrast versus volume filling fraction in the range 0 to 1 is given in Figure 7. We have given a new mechanism of the minimum refractive index difference which when added to the density of states minimum may be useful to assure the occurrence of the photonic band gap due to overlapping of gaps of different BZ. The alternative mechanism of scattering strength is greater than 1.

We have proposed an alternative mechanism of scattering strength, which when greater than one indicates the occurrence of PBG. The optimum scattering strength optimized in this work is given in eq. (20) and minimum dielectric contrast using eq. (30) could be estimated from the variation of refractive index contrast versus volume filling fraction and it is 2.414 as obtained from Figure 7. The relative width using scattering strength concept can be determined at W-point of the BZ using eq. (33). The variation of effective dielectric constant has been discussed. The effective refractive index for W-point of BZ is given in eq. (6) and it may be used to get relative width as in eq.(35) for nematic liquid crystal infiltrated in synthetic opal in Figure 8 and that for ferroelectric liquid crystal infiltrated in opal is given in Figure 9. There is a change of anisotropic behaviour and phase transition as a function of temperature. The Figures 8 and 9 indicate temperature tuning of photonic band gap. Our calculation of effective dielectric constant as a function of filling fraction for spherical air atoms for MG, MMMG, EM theory and experimental data and also for dielectric sphere are given Figure 10. A comparison of our calculated result shows a close agreement with MMMG result.

The lamb shift calculated in this work using eq.(42) taking $\varepsilon_0=1$ and $\varepsilon_0\neq1$ is illustrated in Figure 11. The anomalous Lamb shift in $2p_{1/2}$ level is significantly more than that obtained by using isotropic model which indicates that odd parity $2p_{1/2}$ state of hydrogen is significantly influenced by introducing anisotropic behaviour of BZ.

Our work on band structure for liquid crystal infiltrated opal using an approach of Ho et al is illustrated Figure 12. The Figure 12(a) have been obtained for liquid crystal, when each director of the nematic axis turns at random, i.e., isotropic material and Figure 12(b) is of the

opal infiltrated with liquid crystal, when the director of the nematic axis turns at perpendicular to (1,1,1) director of the light. Figure 12 (a) indicate isotropic situation where 1^{st} and 2^{nd}, 3^{rd} and 4^{th} bands are degenerate. But when the director of the axis turns with an angle the degeneracy is lifted for the case of L-point (1, 1, 1) of the BZ. Now 1^{st} and 2^{nd}, 3^{rd} and 4^{th} bands are separated from each other and they become non-degenerate. There is a gap between 1^{st} and 2^{nd}, 3^{rd} and 4^{th}, the 2^{nd} is biggest under the isotropic conditions of liquid crystal infiltrated opal, while 1^{st} band gap is biggest when degeneracy is lifted due to anisotropy effect.

Conclusion

The work included in this paper provides fruitful information to understand the physical basis of photonic band gap and it may help in fabricating photonic crystal. This paper briefly reviews photonic crystal structure and we report our finding on relative width, filling fraction, effective refractive index, scattering strength, mechanism of PBG, dielectric contrast, Lamb Shift and band structure calculation. The refractive index contrast of 2.414 obtained by us for face centered cubic lattice is the least one till date.

Acknowledgements

We gratefully acknowledge Late Prof. G.K. Johri and Prof. Katsumi Yoshino (Department of Electrical Engineering, Osaka University, Japan) for having fruitful discussions with us on some of these findings. This work was completed within the framework of the Associateship Scheme of the Abdus Salam International Centre for Theoretical Physics awarded to Manoj Johri.

References

1 Anderson P W, *Phys Rev,* 109 (1958) 1492.

2 Purcell E M, *Phys Rev,* 69 (1946) 681.

3 John S, *Phys Rev Lett,* 53 (1984) 2169.

4 John S, *Phys Rev Lett,* 58 (1987) 2486.

5 Yablonovitch E, *Phys Rev Lett,* 58 (1987) 2059.

6 Yablonovitch E and Gmitter T J, *Phys Rev Lett,* 63 (1989) 1950.

7 Ho K M, Chan C T, and Soukoulis C M, *Phys Rev Lett,* 65 (1990) 3152; Chan C T, Ho K M and Soukoulis C M, *Europhys Lett,* 16 (1991) 563.

8 Yablonovitch E, Gmitter T J, and Leung K M, *Phys Rev Lett,* 67 (1991) 2295.

9 Yablonovitch E., Gmitter T J, Meade R D, Kappe A M, Brommer K D, Joannopoulous J D, *Phys Rev Lett,* 67 (1991) 3380.

10 John S and Wang J, *Phys Rev Lett,* 64 (1990) 2418.

11 John S and Wang J, *Phys Rev B,* 43 (1991) 12772.

12 Yablonovitch E, *Scientific American*, (Dec., 2001) 47.

13 Johri G K, Johri Manoj, Tiwari Akhilesh, Sharma Rajesh and Yoshino Katsumi, *Mol Crys Liq Crys,* 368 (2001) 359.

14 Johri G K, Tiwari Akhilesh, Johri Manoj and Yoshino Katsumi, *Jpn J Appl Phys,* 40 (2001) 4565.

15 Johri G K, Tiwari Akhilesh, Saxena Saumya and Johri Manoj, *Mod Phys lett B*, 15 (2001) 529.

16 Johri G K, Sharma Rajesh, Tiwari Akhilesh, Srivastava Kuldeep, Saxena Saumya and Johri M, *Pramana*, 58 (2002) 563.

17 Johri G K, Tiwari Akhilesh, Johri Manoj, Saxena Saumya and Yoshino Katsumi, *J Soc Elect Mat Eng,* 10 (2001) 269.

18 Johri Gajendra K, Johri Manoj, Tiwari Akhilesh and Yoshino Katsumi, *IEEE TDEI*, 11 (Feb 2004) 184.

19 Leung K M and Liu Y F, *Phys Rev Lett,* 65 (1990) 2646.

20 Sözüer H S, Haus J W, and Inguva R, *Phys Rev B,* 45 (1992) 13962.

21 Zhang Z and Satpathy S, *Phys Rev Lett,* 65 (1990) 2650.

22 Lorentz L, Wiedemannasche Annalen, 11 (1880) 70; Lorentz H A, The Theory of Electrons (Tuebner, Leipzig) 1909: reprint (Dover, NewYork) 1952.

23 Bruggeman D A G, *Ann Phys (Leipzig)* 24 (1935) 636.

24 Korringa J, *Physica (Utrecht)* 13, (1947) 392; Kohnand W, Rostoker N, *Phys Rev* 94 (1954) 111.

25 Leung K M, and Lin Y F, *Phys Rev B,* 41 (1990) 10188.

26 Garnett Maxwell J C, *Philos. Trans. R. Soc. London,* 203 (1904) 385.

27 Busch K and Soukoulis C M, *Phys Rev Lett,* 75 (1995) 3442.

28 Lamb W E and Retherford, *Phys Rev* 72 (1947) 241.

29 Quang T, Woldeyohannes M, John S and Agrawal G S, *Phys Rev Lett* 79 (1997) 5238.

30 Takeda H and Yoshino K, *J Soc Elect Mat Eng,* 10 (2001) 119.

Table 1 Optimal values of refractive index contrast, volume filling fraction, size of the gap in the Photonic crystals in three dimensional fcc dielectric crystal structure.

n_a/n_b	filling fraction(f)	$\Delta\omega/\omega_0$	Remark and Ref.
1.46	—	—	Spherical atom and closed packed lattice(pseudogap theoretical)[4]
3.6	0.37	15.7%	Diamond lattice full PBG non-spherical (theoretical)[7]
3.6	0.81	28.8%	″ ″
2.0	0.34(air)	46%	″ ″
2.0	0.81(diel.)	21%	″ ″
3.6	0.78	19%	Cylindrical microstructure closed packed (experimental)[7]
2.1	—	—	Normalized hole diameter ≈ 0.469 (Ref.7)
1.6	0.11	—	Spherical atom and closed packed lattice(experimental)[8]
3.5	0.15	6.7%	″ ″
3.03	0.16	6.7%	″ ″
3.03	0.67	0.0	″ ″
2.8	0.10 to 0.15	13%	Largest band gap[23]
4.6	—	9.5%	Saturated (theoretical)[24]

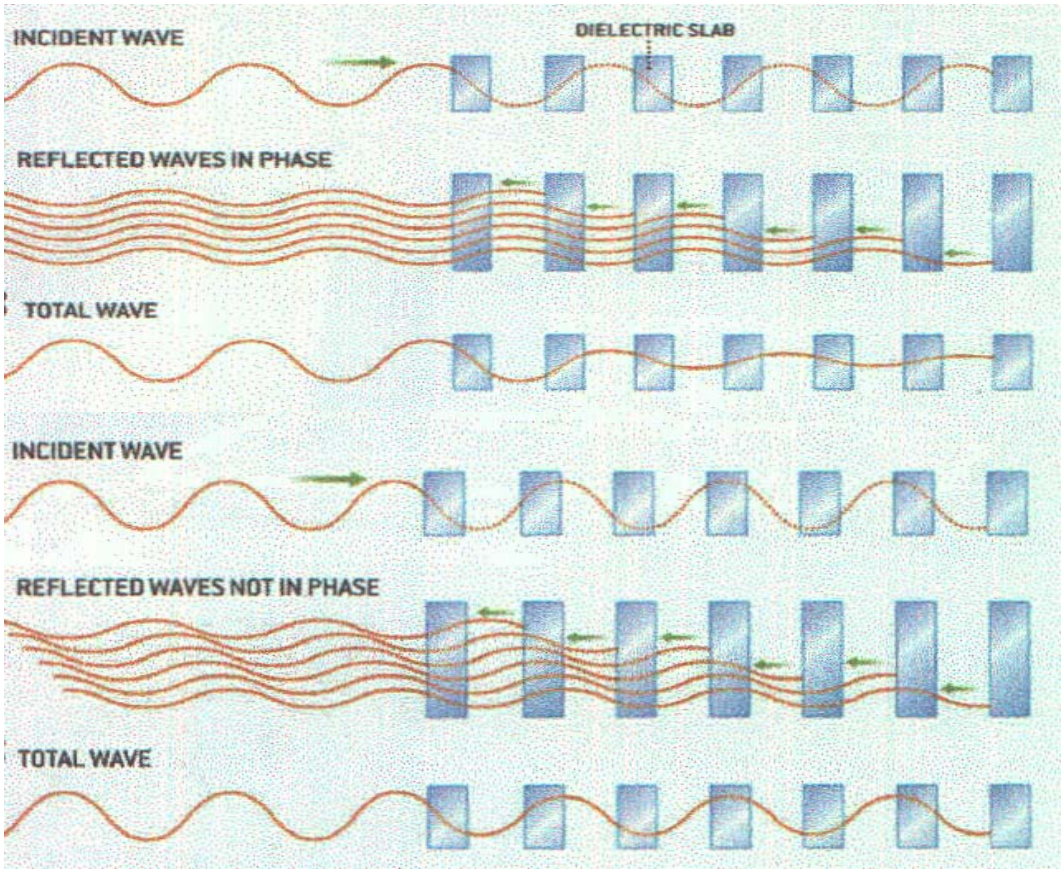

Figure 1(a, b, c) One dimension for wavelength in band gap and 1(d, e, f) for wavelength not in band gap

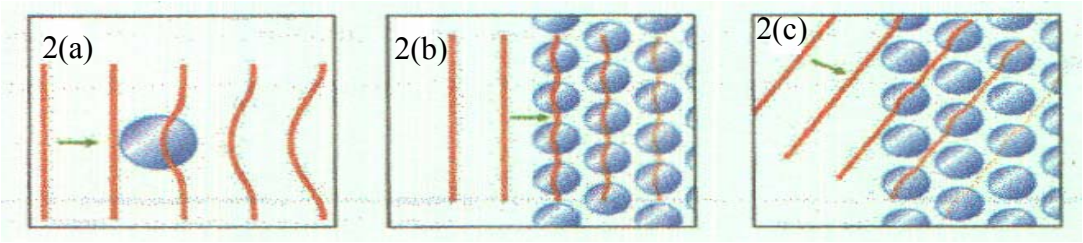

Figure 2(a, b, c) Two Dimensions

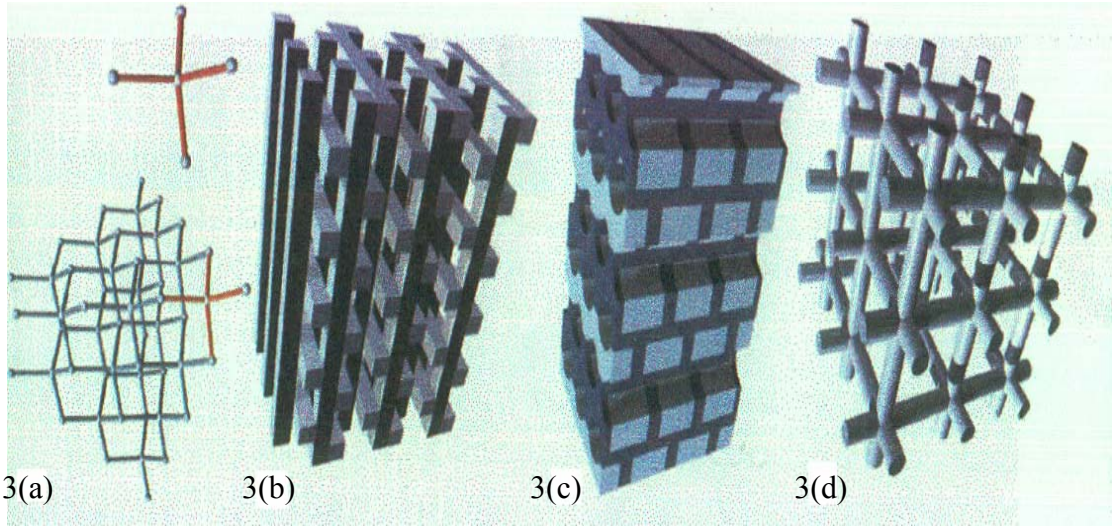

Figure 3(a, b, c) Three Dimensions

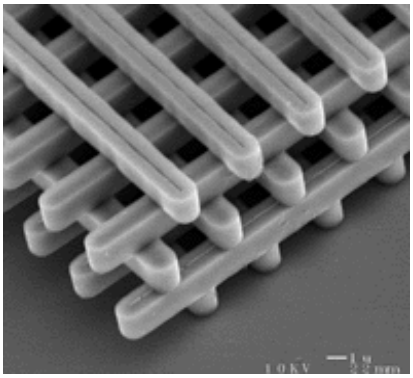

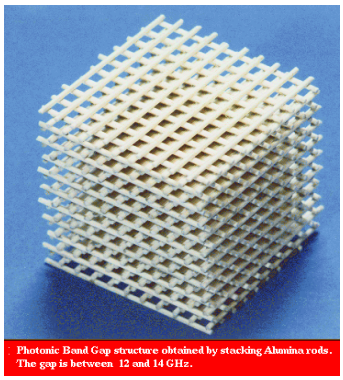

Woodpile Structures

S. Lin, Sandia National Lab

Soukoulis Group, Iowa State University

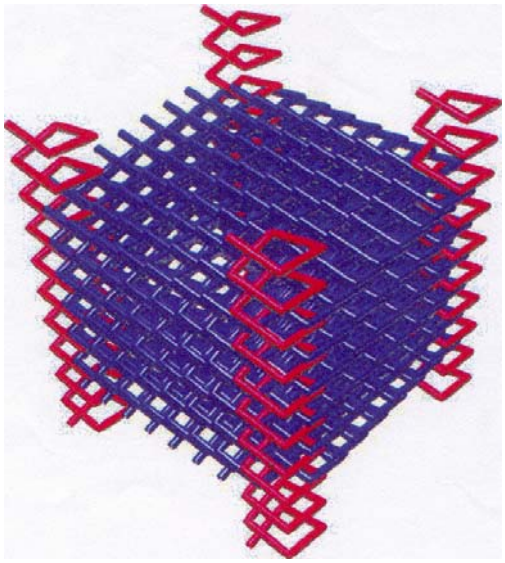

Square Spirals
John's Group, University of Toronto

Figure 4 Some 3-D Structures used by different groups.

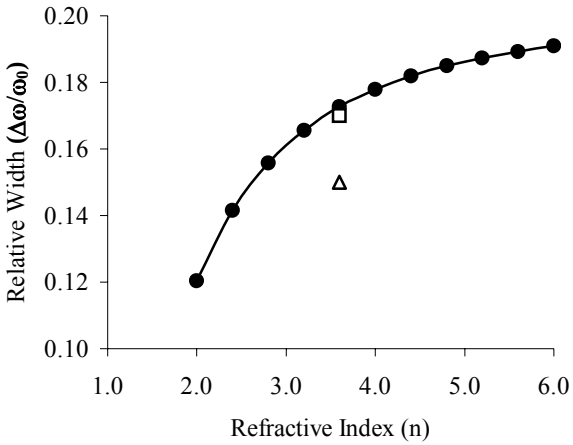

Figure 5 Variation of relative width ($\Delta\omega/\omega_0$) with refractive index (n) for Eq (1); □ For Yablonovitch; Δ for Ho et al.

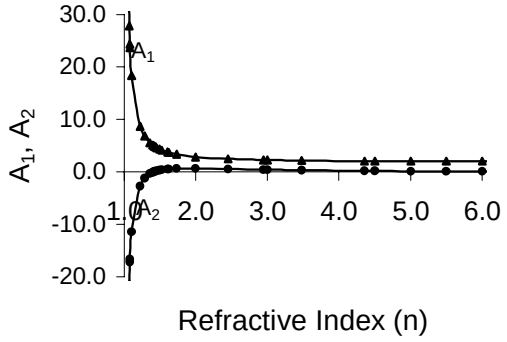

Figure 6 Variation of coefficients $\boldsymbol{A}_1$, $\boldsymbol{A}_2$, occurred as in fluctuating potential in eq (11) as a function of refractive index contrast ($n_a/n=n$, $n_b=1$).

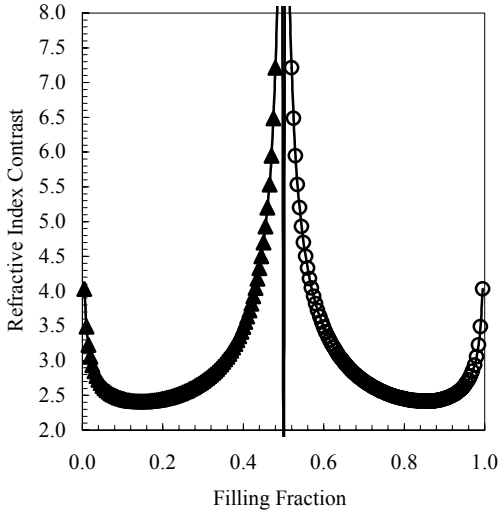

Figure 7 Variation of refractive index contrast versus volume filling fraction in the range 0 to 1 with filled triangles for n_a/n_b and hollow circles for n_b/n_a.

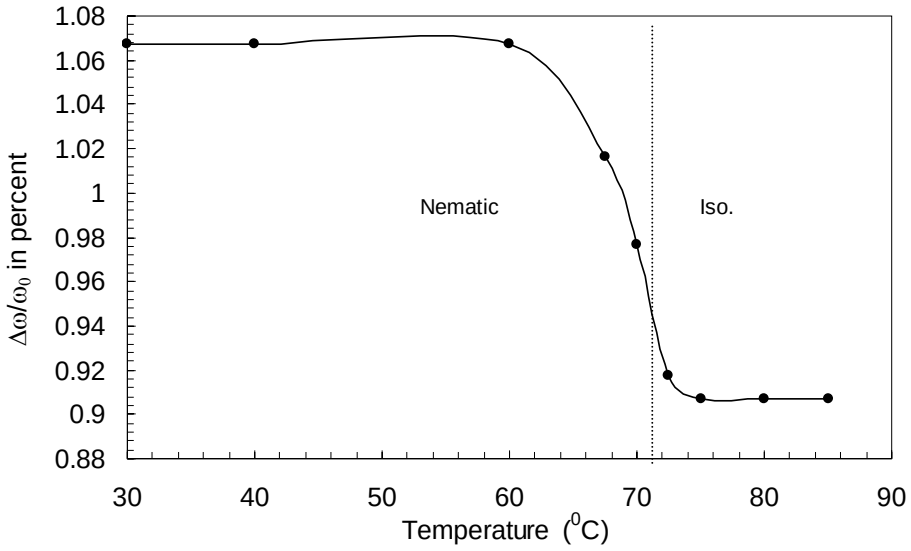

Figure 8 Temperature dependence of calculated relative width ($\Delta\omega/\omega_c$) of nematic liquid crystal ZLI-1132

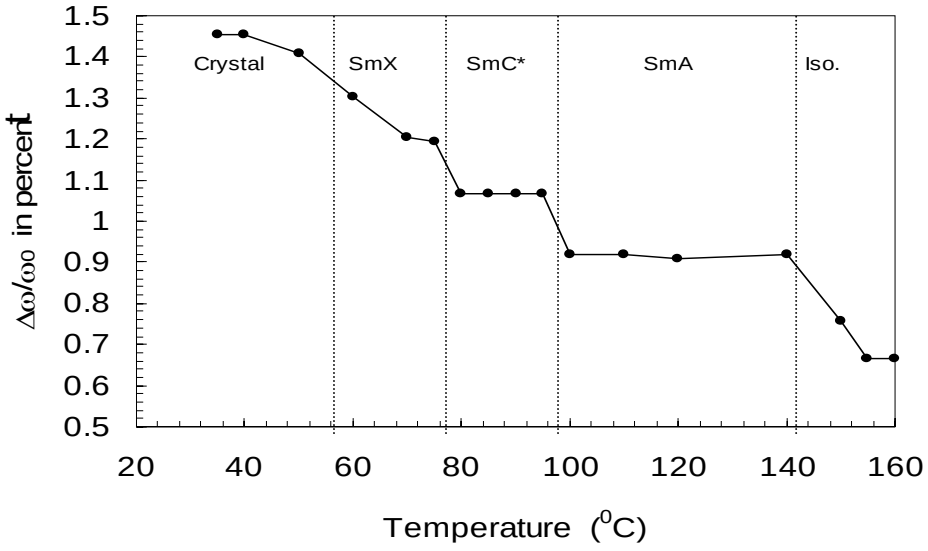

Figure 9 Temperature dependence of calculated relative width ($\Delta\omega/\omega_0$) of ferroelectric liquid crystal 1MC1EPOPB.

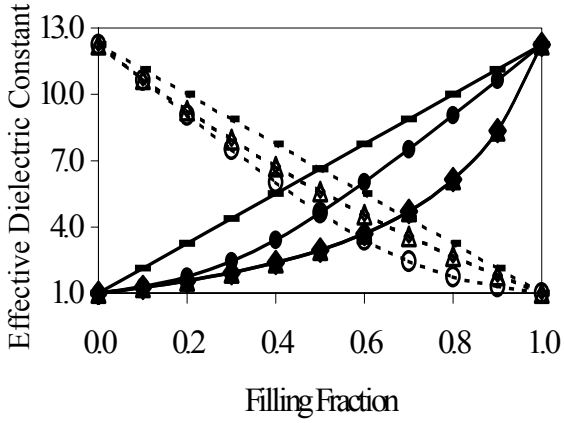

Figure 10 Variation of effective dielectric constant with filling fraction for spherical air atoms (6) MG result, (Σ) MMMG result (λ) EM theory, (−) Experimental result[6], and for dielectric sphere (◊) MG result, (Δ) MMMG result, (O) EM theory, (-) Experimental result.

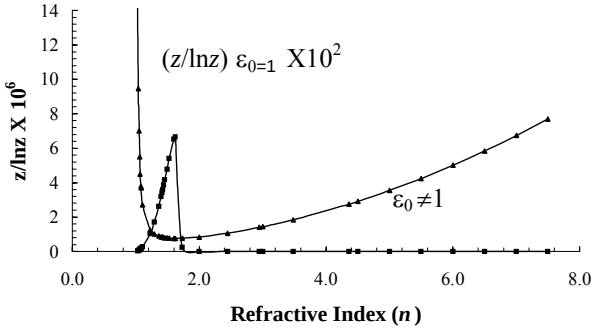

Figure 11 Variation of z/lnz for different values of ε_0 and for $\varepsilon_0=1$ assumed elsewhere[28] with refractive index contrast. The values of z/lnz for $\varepsilon_0=1$ have been multiplied by 100 to show them in this diagram

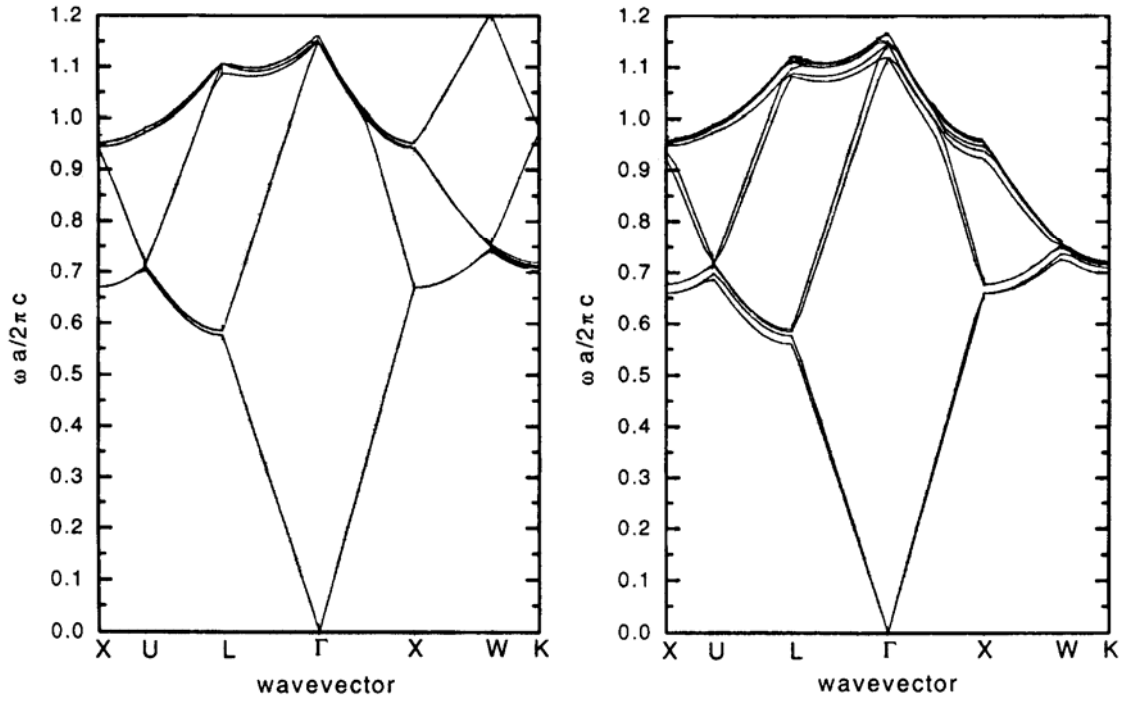

Figure 12 (a) Dispersion curve of the opal (n_{opal} =1.46) infiltrated with liquid crystal (n_{LC}=1.584) when each director of the nematic axis turns at random, i.e., isotropic material. (b) Dispersion curve of the opal (n_{opal}=1.46) infiltrated with liquid crystal crystal (n_{LC}=1.584) when each director of the nematic axis turns at $\phi=\pi/4$ and $\theta=-\pi/2+\cos^{-1}(1/\sqrt{3})$, i.e., it is perpendicular to (1,1,1) director of the light.